Chem Biol Drug Des 2013; **82:** 125–130

Research Article

Design and Synthesis of a Tetrahydroisoquinoline-Based Hydroxamate Derivative (ZYJ-34v), An Oral Active Histone Deacetylase Inhibitor with Potent Antitumor Activity

Yingjie Zhang[1], Chunxi Liu[2], C. James Chou[3], Xuejian Wang[4], Yuping Jia[5] and Wenfang Xu[1,*]

[1]Department of Medicinal Chemistry, School of Pharmacy, Shandong University, Ji'nan, Shandong, 250012, China
[2]Department of Pharmaceutics, School of Pharmacy, Shandong University, Ji'nan, Shandong, 250012, China
[3]Department of Drug Discovery and Biomedical Sciences, South Carolina College of Pharmacy, Medical University of South Carolina, Charleston, SC, 29425, USA
[4]Postdoctoral Workstation, Weifang Biomedical Industry Park Management Office, Weifang, Shandong, 261205, China
[5]Key Laboratory of Chemical Drugs, Shandong Institute of Pharmaceutical Industry, Jinan, Shandong, 250101, China
**Corresponding author: Wenfang Xu, wfxu@yahoo.cn*

In our previous study, we developed a novel series of tetrahydroisoquinoline-based hydroxamic acid derivatives as histone deacetylase inhibitors (*Bioorg Med Chem*, 2010, 18, 1761–1772; *J Med Chem*, 2011, 54, 2823–2838), among which, compound ZYJ-34c (1) was identified and validated as the most potent one with marked in vitro and in vivo antitumor potency (J Med Chem, 2011, 54, 5532–5539.). Herein, further modification in 1 afforded another oral active analog ZYJ-34v (2) with simplified structure and lower molecular weight. Biological evaluation of compound 2 showed efficacious inhibition against histone deacetylase 1, 2, 3, and 6, which was confirmed by Western blot analysis results. Most importantly, compound 2 exhibited similar even more potent in vitro and in vivo antitumor activities relative to the approved histone deacetylase inhibitor SAHA.

Key words: antitumor, histone deacetylases, inhibitor, oral active, tetrahydroisoquinoline, valproic acid

Abbreviations: CDK, cyclin-dependent kinase; HDAC, histone deacetylase; HDACIs, histone deacetylase inhibitors; VPA, valproic acid; ZBG, zinc-binding group.

Received 10 December 2012, revised 6 March 2013 and accepted for publication 2 April 2013

Epigenetic covalent modifications of histone and DNA dramatically affect gene expression and cellular activity, and epigenetic disorder could lead to many diseases, especially cancer. Generally, epigenetic modifications are reversible, catalyzed by pairs of enzymes with converse activity. Among these enzymes, histone deacetylases (HDACs) have attracted the most attention over the past decades (1).

Histone deacetylase are amidohydrolases with multiple functions. In cell nuclear, HDACs catalyze the deacetylation of lysine residues located at the *N*-terminal of nucleosomal histones, which results in condensed chromosomal DNA and transcriptional repression (2–4). Over the past few years, kinds of non-histone proteins involved in cell growth and survival pathways have been identified as HDAC substrates, such as transcription factors, cytoskeletal proteins, molecular chaperones, and nuclear import factors (5).

Eighteen HDAC isoforms, grouped into four classes, are encoded in the human genome. The enzymes of classes I (HDACs 1–3 and 8), II (HDACs 4–7, 9 and 10), and IV (HDAC 11) are Zn^{2+}-dependent metallohydrolases, whereas the class III HDACs (sirtuins 1–7) utilize NAD^+ as a cofactor. It has been revealed that Zn^{2+}-dependent isozymes, especially class I and class II HDACs, are involved in tumorigenesis and development, and inhibition of these isoforms could result in proliferation inhibition, cellular differentiation, apoptosis, susceptibility to chemotherapy, antiangiogenesis, and migration inhibition of tumor cells (6). In this context, categories of histone deacetylase inhibitors (HDACI) against Zn^{2+}-dependent HDACs have been developed. Currently, over 20 HDACI are in clinical trials as antitumor agents and two of them, SAHA (Figure 1) and FK228 (Figure 1), are already on the market (7).

Most HDAC inhibitors, including the intracellular active form of FK228 (Figure 1), share a common pharmacophore consisting of three domains: a zinc-binding group (ZBG) that co-ordinates to the catalytic Zn^{2+} at the bottom of the active site, a cap group able to interact with the rim of active site entrance, and a linker that occupies the active site tunnel and tethers ZBG to cap (Figure 1).

 doi: 10.1111/cbdd.12144

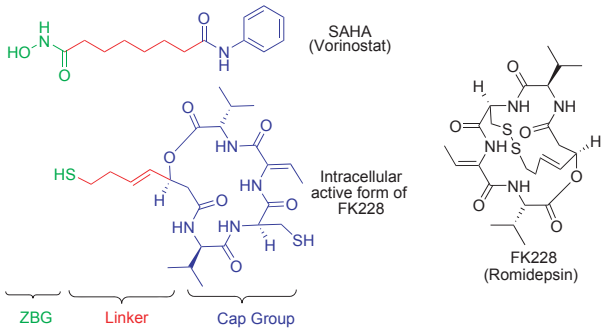

Figure 1: The structures of SAHA and FK228 and the common pharmacophore of histone deacetylase (HDACs) inhibitor.

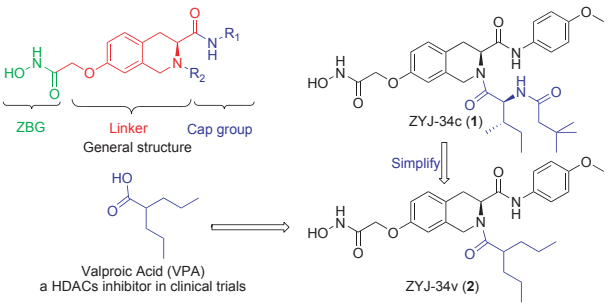

Figure 2: General structure of tetrahydroisoquinoline-based histone deacetylase (HDACs) inhibitor and the design idea of target compound ZYJ-34v.

According to the HDACI pharmacophore, we previously designed and synthesized a novel series of tetrahydroisoquinoline-based hydroxamate derivatives as HDACI (Figure 2) (8–10). Among these analogs, compound ZYJ-34c (**1**, Figure 2) was identified and validated as the most potent one with marked *in vitro* and *in vivo* antitumor potency through several rounds of structural optimization and activity screening (10). In the present study, compound ZYJ-34v (**2**, Figure 2) was designed and synthesized by replacing the R_2 group of **1** with the valproyl group. There are three reasons for us to attempt this replacement:

• Valproic acid (VPA) is a HDACI in clinical trials. Considering its hydroxamic acid analog, valpropylhydroxamic acid exhibited lower class I HDACs inhibitory activity compared with VPA (11); we hypothesized that VPA inhibited HDACs by its valproyl group binding with HDACs rather than by its carboxylic acid group chelating with Zn^{2+}. The binding site of VPA in HDACs might be the same binding site of other co-factors. Therefore, VPA could prevent HDACs from interaction with other proteins and the subsequent formation of multiprotein complex, which are crucial for the function of HDACs (6). Moreover, VPA may possibly act as an allosteric inhibitor of HDACs. Based on the above hypothesis, we hoped that the introduction of valproyl group could increase the affinity between **2** and HDACs.

• There is a possibility that the *in vivo* or intracellular partial hydrolysis of **2** could release free VPA and compound **3** (Figure 3), which was identified as a moderately potent HDACI in our previous research (8). If so, there will be three active components (unhydrolyzed ZYJ-34v, VPA, and compound **3**) performing multiple antitumor effects.

• Compared with **1**, compound **2** possesses simplified structure, less chiral center, and lower molecular weight, which are beneficial to its further research and development.

Compound **2** was evaluated against HDAC1, 2, 3, 6 using Boc-Lys (acetyl)-4-amino-7-methylcoumarin substrate and against MDA-MB-231 cell lysate using Boc-Lys (trifluoroacetyl)-4-amino-7-methylcoumarin substrate to profile its HDACs inhibitory activity and selectivity. Western blot analysis and *in vitro* antiproliferative assays were performed to validate its intracellular HDACs inhibitory activity. Moreover, *in vivo* antitumor activity of **2** was assessed in a human breast carcinoma (MDA-MB-231) xenograft model. SAHA was used as reference drug in all above-mentioned assays.

Methods and Materials

Chemistry

Compound **2** was synthesized following the procedures described in Scheme 1. The starting material compound **4** could be smoothly obtained according to our previously published methods (9). Acylation of **4** with VPA and subsequent treatment with NH_2OK led to the target compound **2** (Scheme 1).

In vitro *HDACs inhibition fluorescence assay*

The HDACs inhibition fluorescence assays were conducted by the similar method as previously described (9).

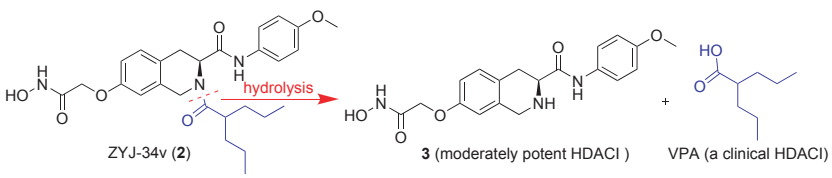

Figure 3: Two possible hydrolytic metabolites of ZYJ-34v.

Boc-Lys (acetyl)-4-amino-7-methylcoumarin substrate was used in inhibition assays against class I (HDAC1, HDAC2, HDAC3) and class IIb (HDAC6), while Boc-Lys (trifluoroacetyl)-4-amino-7-methylcoumarin substrate for class IIa (MDA-MB-231 cell lysate). In brief, 10 μL of enzyme solution was mixed with various concentrations of tested compound (50 μL). Five minutes later, 40 μL of fluorogenic substrate was added, and the mixture was incubated at 37 °C for 30 min and then stopped by addition of 100 μL of developer containing trypsin and TSA. After incubation at 37 °C for 20 min, fluorescence intensity was measured using a microplate reader at excitation and emission wavelengths of 390 and 460 nm, respectively. The inhibition ratios were calculated from the fluorescence intensity readings of tested wells relative to those of control wells, and the IC_{50} values were calculated using a regression analysis of the concentration/inhibition data.

In vitro *antiproliferative assay*

In vitro antiproliferative assay was determined by the MTT (3-[4,5-dimethyl-2-thiazolyl]-2,5-diphenyl-2*H*-tetrazolium bromide) method as previously described (9). Briefly, all cell lines were maintained in RPMI1640 medium containing 10% FBS at 37 °C in 5% CO_2 humidified incubator. Cells were passaged the day before dosing into a 96-well cell plate, allowed to grow for a minimum of 4 h prior to addition of compounds. After compounds addition, the plates were incubated for an additional 48 h, and then 0.5% MTT solution was added. After further incubation for 4 h, formazan formed from MTT was extracted by DMSO for 15 min. Absorbance was then determined using an ELISA reader at 570 nm and the IC_{50} values were calculated according to the inhibition ratios.

Western blot analysis

For Western blot analysis of acetylated tubulin, acetylated histone H3, H4, and p21, total protein extracts were separated on a polyacrylamide gel, transferred onto polyvinylidene difluoride membranes and blotted as previously described (12). Protein immunoblots were shown for acetylated tubulin (Sigma, Shanghai, China), acetylated histone H3 (Sigma), acetylated histone H4 (Sigma), and p21 (Cell Signaling, Shanghai, China) using β-Actin (Sigma) as a loading control.

In vivo *MDA-MB-231 xenograft models*

In vivo MDA-MB-231 xenograft model was established as previously described (9). In brief, conventionally cultured MDA-MB-231 cells were inoculated subcutaneously in the right flanks of female athymic nude mice (BALB/c-nu, 5–6 weeks old, Slac Laboratory Animal, Shanghai, China). About 10 days after injection, tumors were palpable (about 100 mm^3) and mice were randomized into treatment and control groups (seven mice per group). The treatment groups received 90 mg/kg of compound **2** or SAHA by oral gavage for 22 consecutive days, and the blank control group received an equal volume of PBS solution containing DMSO. During treatment, subcutaneous tumor volume and body weight were monitored regularly. After treatment, mice were killed and dissected to weigh the tumor tissues, livers, and spleens. All the obtained data were used to evaluate the antitumor potency and toxicity of compounds. Data were analyzed by Student's two-tailed *t*-test. A *P* level <0.05 was considered statistically significant.

Results and Discussions

Chemistry

All reactions were monitored by TLC with 0.25-mm silica gel plates (60GF-254). UV light, iodine stain, and ferric chloride were used to visualize the spots. Silica gel or C18 silica gel was used for column chromatography purification. All commercially available starting materials, reagents, and solvents were used without further purification unless otherwise stated. Melting points were determined uncorrected on an electrothermal melting point apparatus. ^{1}H NMR spectra were recorded on a Bruker DRX spectrometer at 600 MHz, δ in parts per million and *J* in hertz, using TMS as an internal standard. High-resolution mass spectra were conducted by Shandong Analysis and Test Center in Ji'nan, China. ESI-MS spectra were recorded on an API 4000 spectrometer. Compound **2** are >95% pure by HPLC analysis, performed on a Agilent 1100 HPLC instrument using a Phenomenex Synergi 4μ Polar-RP 80A column (250 mm × 4.6 mm), eluted with 50% acetonitrile/50% water (containing 0.1% formic acid) over 30 min, with detection at 254 nm and a flow rate of 1.0 mL/min.

(*S*)-Methyl 2-((3-((4-methoxyphenyl)carbamoyl)-1,2,3,4-tetrahydroisoquinolin-7-yl)oxy)acetate (**4**) was synthesized according to the methods in our previous study (9).

(*S*)-7-(2-(hydroxyamino)-2-oxoethoxy)-*N*-(4-methoxyphenyl)-2-(2-propylpentanoyl)-1,2,3,4-tetrahydroisoquinoline-3-carboxamide **(2)**. At room temperature, to a solution of VPA (**5**) (1.32 g, 9.2 mmol) in anhydrous THF (40 mL), was added Et_3N (1.02 g, 10 mmol) followed by 2-(1*H*-benzotriazole-1-yl)-1,1,3,3-tetramethyluronium tetrafluoroborate (TBTU, 3.24 g, 10 mmol). After 15 min, the amine compound **4** (3.33 g, 9.0 mmol) was added. Stirring was continued until compound **4** disappeared by TLC, then THF was evaporated with the residue being taken up in EtOAc (50 mL). The EtOAc solution was washed with saturated Na_2CO_3 (3 × 10 mL), 1 N HCl (3 × 10 mL) and brine (3 × 10 mL), dried over $MgSO_4$, and evaporated under vacuum. The obtained crude product was treated with a solution of NH_2OK in anhydrous methanol for 1 h, and then the solvent was evaporated under vacuum. The residue was acidified with 2 N HCl until pH 5–6 and then extracted with EtOAc (3 × 30 mL). The organic layers were combined, washed with brine (3 × 20 mL), dried over $MgSO_4$, and evaporated with the residue being purified by C18 reversed-

phase column chromatography (H_2O/MeOH 3:7) to give desired compound **2** (1.75 g, 39% yield) as a white powder. Mp: 96–98 °C. ^{1}H-NMR (DMSO-d_6, 600 MHz) δ 0.67–0.89 (m, 6H, $CH_3CH_2CH_2CHCH_2CH_2CH_3$), 1.06–1.55 (m, 8H, $CH_3CH_2CH_2CHCH_2CH_2CH_3$), 2.96–3.17 (m, 3H, CH_2CHCH_2 and $PhCH_2CH$), 3.70 (s, 3H, OCH_3), 4.45 (s, 2H, OCH_2CO), 4.49–4.94 (m, 3H, NCHCO and $PhCH_2N$), 6.74–6.92 (m, 4H, benzene protons), 7.11–7.15 (m, 1H, benzene proton), 7.36–7.42 (m, 2H, benzene protons), 8.96 (s, 1H, NHOH), 9.88 (s, 1H, PhNH), 10.82 (s, 1H, NHOH). HRMS (AP-ESI) *m/z* calculated for $C_{27}H_{36}N_3O_6$ $[M + H]^+$ 498.2604, found 498.2611. Retention time: 6.3 min.

HDACs inhibition assay

To compare their HDACs inhibitory activity and isoform selectivity, compound **2** and SAHA were tested against HDAC1, HDAC2, HDAC3, and HDAC6 using acetylated substrate. Besides, the class IIa inhibitory activity was evaluated against MDA-MB-231 cell lysate using class IIa-specific triflouroacetylated substrate (13). Results listed in Table 1 showed that compared to SAHA compound **2** exhibited superior inhibitory capacities against HDAC1 and HDAC2, while inferior inhibitory capacities against HDAC3 and HDAC6. Neither compound **2** nor SAHA exhibited obvious inhibition against class IIa HDACs up to 10 μM, which was consistent with literature information that SAHA was not active against class IIa HDACs (14). Overall, compound **2** was equipotent to SAHA.

Western blot analysis

We also confirmed that compound **2** was cell permeable and able to inhibit intracellular even nuclear HDACs by monitoring the acetylation levels of tubulin, histones H3 and H4 in MDA-MB-231 cell line. Acetylated tubulin is a known target of HDAC6, and histones are the common targets of HDAC1 and HDAC2. Moreover, the effect on the expression level of the cyclin-dependent kinase inhibitor p21 was also investigated. Silencing of the tumor suppressor gene *p21* through hypoacetylation is a hallmark of many cancers, and HDACs inhibition in the nucleus could induce apoptosis via re-establishing expression of p21 (15). As indicated in Figure 4, both compound **2** and SAHA effectively inhibited deacetylation of tubulin, histone H3 and H4, and significantly induced increase in the protein level of p21 at 1 μM after 24 h of treatment.

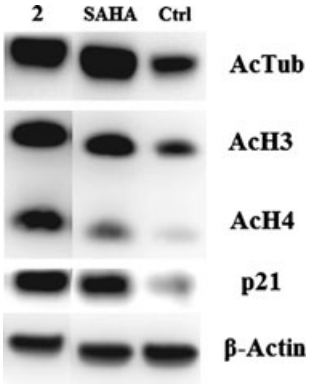

Figure 4: Western blot analysis of acetylated tubulin, acetylated histone H3, acetylated histone H4 and p21 in MDA-MB-231 cell lines after 24 h treatment with compounds at 1 μM. β-Actin was used as a loading control.

Table 2: Antiproliferative activity of compound **2** with SAHA as positive control

	IC_{50} (μM)[a]				
Compound	MDA-MB-231	HCT116	PC-3	HepG2	MCF-7
2	1.41	0.63	2.62	4.23	4.76
SAHA	1.52	0.60	3.97	6.29	3.44

[a]Values are the mean of three experiments. The standard derivations are <20% of the mean.

In vitro *antiproliferative activity assay*

The potent HDACs inhibitory activities of compound **2** promoted us to evaluate its *in vitro* antiproliferative activity against several tumor cell lines (Table 2). Overall, the antiproliferative activity of compound **2** was similar even superior to that of SAHA, which correlated well with aforementioned biological test results.

In vivo *antitumor activity assay*

Encouraged by its promising *in vitro* activity, the *in vivo* antitumor potency of compound **2** was evaluated in a subcutaneous MDA-MB-231 xenograft model. Tumor growth inhibition (TGI) and relative increment ratio (T/C) were used as the evaluation indicators to reveal the antitumor effects in tumor weight and tumor volume, respectively.

	Class I			Class IIb	Class IIa
Compound	HDAC1	HDAC2	HDAC3	HDAC6	Cell lysate
2	37.6 ± 12.1	174.8 ± 6.2	87.7 ± 11.7	675 ± 125	NA[b]
SAHA	75.6 ± 11.1	256.4 ± 2.1	28.4 ± 11.2	118 ± 11.9	NA[b]

[a]Assays were performed in replicate ($n \geq 2$); IC_{50} (nM) values are shown as mean ± SD.
[b]NA: not active at 10 μM.

Table 1: Histone deacetylase (HDACs) inhibitory activity and isoform selectivity of compound **2** and SAHA[a]

Table 3: Effects of compounds on a mouse MDA-MB-231 xenograft model

Compound	Body weight (g)	Liver weight (g)	Spleen weight (g)	TGI[a]	T/C[a]
Blank control	25.37 ± 1.27	2.1 ± 0.43	0.2 ± 0.07	–	–
SAHA (90 mg/kg, po)	23.23 ± 2.08	1.69 ± 0.2	0.17 ± 0.06	56%	52%
2 (90 mg/kg, po)	25.61 ± 1.41	1.67 ± 0.58	0.16 ± 0.06	59%	49%

TGI, tumor growth inhibition.
[a]Compared with the control group, all treated groups showed statistically significant ($P < 0.05$) TGI and T/C by Student's two-tailed *t*-test.

Tumor growth inhibition = (the mean tumor weight of control group – the mean tumor weight of treated group)/the mean tumor weight of control group.

Tumor volume (V) was estimated using the equation ($V = ab^2/2$, where a and b stand for the longest and shortest diameter, respectively). T/C was calculated according to the following formula:

T/C =the mean RTV of treated group
/the mean RTV of control group

RTV, namely relative tumor volume = V_t/V_0, (V_t: the tumor volume measured at the end of treatment; V_0: the tumor volume measured at the beginning of treatment).

The data present in Table 3 tumor growth curve (Figure 5A) and the final tumor volume (Figure 5B) showed that compound **2** (TGI = 59%, T/C = 49%) possessed comparable *in vivo* antitumor activity to the approved drug SAHA (TGI = 56%, T/C = 52%). According to the final body weight and the dissected liver and spleen weight of treated mice (Table 3), there was no evidence that compound **2** was more toxic than SAHA. In fact, during experiment no obvious body weight loss was detected in mice treated by compound **2**.

Conclusion and Future Directions

Structural modification in our previously discovered potent HDACI compound **1** led to another oral active HDACI compound **2** with efficacious inhibitory activity against HDAC1, HDAC2, HDAC3, and HDAC6. Compared with the approved HDACI SAHA, compound **2** exhibited similar even superior *in vitro* antiproliferative activity and *in vivo* antitumor potency in a MDA-MB-231 xenograft model. Compared with its parent compound **1**, compound **2** possesses more convenient synthetic route and less chiral center, which facilitates its further research and development as a new drug candidate. Currently, related pharmacokinetic research of compound **2** is underway to find out if VPA could be released by *in vivo* metabolism of compound **2**. On the other hand, the simplified structure and

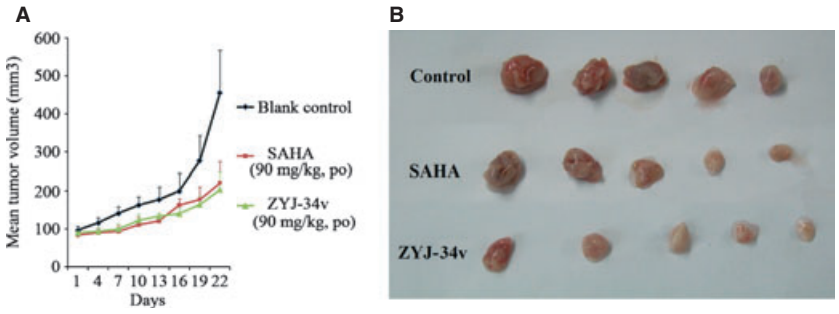

Figure 5: (A) Growth curve of implanted MDA-MB-231 xenograft in nude mice. Data are expressed as the mean ± standard deviation. (B) The picture of dissected MDA-MB-231 tumor tissues. The largest and smallest tumor tissues of every group were omitted.

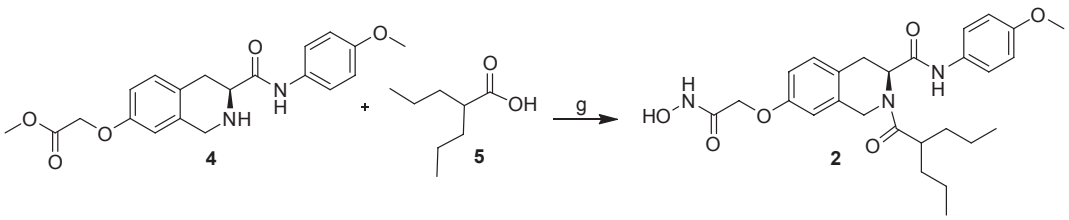

Scheme 1: Reagents and conditions: (a) i). TBTU, Et3N, THF; ii). NH_2OK, CH_3OH, 32% for two steps.

lower molecular weight of compound **2** leave a margin of subsequent structural modification to further increase its activity. We are endeavoring to search more potent HDACI using compound **2** as the lead.

Acknowledgments

This study was supported by National Scientific and Technological Major Project of Ministry of Science and Technology of China (Grant No. 2011ZX09401-015), National Natural Science Foundation of China (Grant No. 21172134), Doctoral Foundation of Ministry of Education of China (Grant No. 20110131110037), Independent Innovation Foundation of Shandong University, IIFSDU (Grant No. 2013GN013), and National Cancer Institute of the National Institute of Health (Award No. R01CA163452).

There is no conflicts of interest.

References

1. Best J.D., Carey N. (2010) Epigenetic opportunities and challenges in cancer. Drug Discov Today;15:65–70.
2. Wolffe A.P. (1996) Histone deacetylase: a regulator of transcription. Science;272:371–372.
3. Hassig C.A., Schreiber S.L. (1997) Nuclear histone acetylases and deacetylases and transcriptional regulation: HATs off to HDACs. Curr Opin Chem Biol;1:300–308.
4. Kouzarides T. (1999) Histone acetylases and deacetylases in cell proliferation. Curr Opin Genet Dev;9:40–48.
5. Glozak M.A., Sengupta N., Zhang X., Seto E. (2005) Acetylation and deacetylation of non-histone proteins. Gene;363:15–23.
6. Witt O., Deubzer H.E., Milde T., Oehme I. (2009) HDAC family: what are the cancer relevant targets? Cancer Lett;277:8–21.
7. Giannini G., Cabri W., Fattorusso C., Rodriquez M. (2012) Histone deacetylase inhibitors in the treatment of cancer: overview and perspectives. Future Med Chem;4:1439–1460.
8. Zhang Y., Feng J., Liu C., Zhang L., Jiao J., Fang H., Su L., Zhang X., Zhang J., Li M., Wang B., Xu W. (2010) Design, synthesis and preliminary activity assay of 1,2,3,4-tetrahydroisoquinoline-3-carboxylic acid derivatives as novel histone deacetylases (HDACs) inhibitors. Bioorg Med Chem;18:1761–1772.
9. Zhang Y., Feng J., Jia Y., Wang X., Zhang L., Liu C., Fang H., Xu W. (2011) Development of tetrahydroisoquinoline-based hydroxamic acid derivatives: potent histone deacetylase inhibitors with marked in vitro and in vivo antitumor activities. J Med Chem;54:2823–2838.
10. Zhang Y., Fang H., Feng J., Jia Y., Wang X., Xu W. (2011) Discovery of a tetrahydroisoquinoline-based hydroxamic acid derivative (ZYJ-34c) as histone deacetylase inhibitor with potent oral antitumor activities. J Med Chem;54:5532–5539.
11. Fass D.M., Shah R., Ghosh B., Hennig K., Norton S., Zhao W.N., Reis S.A., Klein P.S., Mazitschek R., Maglathlin R.L., Lewis T.A., Haggarty S.J. (2011) Short-chain HDAC inhibitors differentially affect vertebrate development and neuronal chromatin. ACS Med Chem Lett;2:39–42.
12. Feng J., Fang H., Wang X., Jia Y., Zhang L., Jiao J., Zhang J., Gu L., Xu W. (2011) Discovery of N-hydroxy-4-(3-phenylpropanamido) benzamide derivative 5j, a novel histone deacetylase inhibitor, as a potential therapeutic agent for human breast cancer. Cancer Biol Ther;11:477–489.
13. Inks E.S., Josey B.J., Jesinkey S.R., Chou C.J. (2012) A novel class of small molecule inhibitors of HDAC6. ACS Chem Biol;7:331–339.
14. Bradner J.E., West N., Grachan M.L., Greenberg E.F., Haggarty S.J., Warnow T., Mazitschek R. (2010) Chemical phylogenetics of histone deacetylases. Nat Chem Biol;6:238–243.
15. Huang B.H., Laban M., Leung C.H., Lee L., Lee C.K., Salto-Tellez M., Raju G.C., Hooi S.C. (2005) Inhibition of histone deacetylase 2 increases apoptosis and p21Cip1/WAF1 expression, independent of histone deacetylase 1. Cell Death Differ;12:395–404.